



## INDO AMERICAN JOURNAL OF PHARMACEUTICAL RESEARCH



### DEVELOPMENT OF ROPINIROLE LOADED SYNTHESIZED OCTANOYL AND PALMITOYL CHITOSAN NANOPARTICLES: OPTIMIZATION BY FACTORIAL DESIGN

Prasad R Deshmukh\*, S S Khadabadi

Government College of Pharmacy, Amravati.

#### ARTICLE INFO

##### Article history

Received 05/06/2020

Available online

31/07/2020

##### Keywords

N-Octanoyl Chitosan,

N-Palmitoyl Chitosan,

Ropinirole Hcl,

Iontropic Method,

Factorial Design.

#### ABSTRACT

N-Octanoyl chitosan (NOC) and N-Palmitoyl chitosan (NPC) were synthesized to modified chitosan hydrophobically and characterized by FTIR, NMR, XRD, modified chitosan were having about 14 % degree of substitution and improvement in solubility in solvent. Full  $3^2$  factorial designs were used to optimize ionotropic method to prepared ropinirole loaded nanoparticle of chitosan and modified chitosan. Concentration of N-acyl chitosan, TPP and stirring speed was independent parameter while mean particle size and entrapment were dependent variable. 3D surface plot and counter plot of optimized batch was draw. Average particle size, drug loading and entrapment efficiency of ropinirole loaded nanoparticle was  $150.7 \pm 3.3$  nm,  $24.80 \pm 1.1\%$  and  $54.96 \pm 3.8\%$  respectively which were correlated with increases bulkiness of the acyl substitution in the modified chitosan while zeta potential was found inversely correlated. TEM and SEM imaging relieved spherical structure of nanoparticle. In vitro release of ropinirole in 1.2 pH HCl buffer and pH 7.4 phosphate buffer showed biphasic release pattern best fitted with Korsmeyer-Peppas kinetics with fickian transport mechanism. Acylated chitosan showed enhancement of sustained release with increasing length of acyl group. Result of the present study showed that hydrophobically modified acylated chitosan can be useful for achieving sustained release controlled by acylation modification.

#### Corresponding author

##### Prasad R Deshmukh

Government College of Pharmacy, Amravati

prasad.deshmukh37@gmail.com

Please cite this article in press as **Prasad R Deshmukh** et al. Development of Ropinirole Loaded Synthesized Octanoyl and Palmitoyl Chitosan Nanoparticles: Optimization by Factorial Design. *Indo American Journal of Pharmaceutical Research*. 2020; 10(07).

Copy right © 2020 This is an Open Access article distributed under the terms of the Indo American journal of Pharmaceutical Research, which permits unrestricted use, distribution, and reproduction in any medium, provided the original work is properly cited.

## INTRODUCTION

Chitosan obtain from deacetylation of chitin have biocompatible, biodegradable, mucoadhesive, and non-toxic natures because of its use as a nano carrier has been regularly increased<sup>[1-3]</sup>. Its having hydrophilicity and high solubility in an acidic environment promotes the ready degradation of the chitosan in the harsh acidic environment of the stomach, proteolytic breakdown in the gastrointestinal tract, and poor permeability across the gastrointestinal mucosa because of produces limitation for used as sustain release Nano carriers for oral delivery<sup>[4]</sup>.

Modification such as acylation, alkylation, quatenization, thiolation, sulfation, phosphorylation, and graft copolymerization to chitosan can be because of presence a reactive amino group at C2, hydroxyl groups at C3 and C6 per glucosamine subunit<sup>[5]</sup>. Hydrophobically modified by cholesterol, 5b cholanic acid, tocopherol, galactosylated O-carboxymethyl grafting with stearic acid, N-octyl-O-sulfate-modified are among the evaluated carriers to deliver drugs with sustainable release<sup>[6-10]</sup>.

In this study, chitosan was modified using Octanoyl chloride and Palmitoyl chloride and characterized using Fourier transform infrared spectroscopy (FTIR), <sup>1</sup>H-nuclear magnetic resonance (NMR) spectroscopy, XRD, solubility in solvents and degree of substitution. Optimization of ionotropic method by Full 3<sup>2</sup> factorial designs. Ropinirole HCl loaded nanoparticles of modified N-Acyl chitosan were prepared and evaluated by particle size, zeta potential, PDI, TEM and SEM. Drug loading and *In-Vitro* drug release and released kinetics was also investigated.

## MATERIAL

Chitosan (55kDa; DDA 81.41%) was purchased from Merck while Butyryl chloride from sigma and Lauroyl Chloride from TCI. Ropinirole HCl was obtained as a gift sample from Glenmark Pharmaceutical Ltd (Mumbai, India). All other reagents were of analytical grade and used without further purification.

## METHOD

### Synthesis and Characterization of N Acyl Chitosan

For synthesis, 2.0 g chitosan was dissolved in 100 ml mixing solution of 0.6% (w/v) acetic acid solution and 85 ml of methanol. A molar equivalent (1.2) of Acyl Chloride include Octanoyl Chloride (C<sub>8</sub>H<sub>15</sub>OCl, Mol Wt.=162.66g and Palmitoyl Chloride (C<sub>16</sub>H<sub>31</sub>OCl, Mol Wt.=274.87g) were separately added slowly to the chitosan solution with magnetic stirring for 5 h, respectively. The mixtures were poured into the same volume of methanol and ammonia solution in volume ratio of 7 to 3. The precipitates were filtered and rinsed with distilled water, methanol, and ether. Then, they were dried in a vacuum at 50<sup>0</sup>C overnight<sup>[11]</sup>.

Characterization of synthesize N-Acyl chitosans were carried out by FTIR, NMR, XRD, solubility in solvents, Degree of Substitution using Ninhydrin Assay<sup>[12]</sup>.

### Preparation of chitosan nanoparticles by Ionotropic Gelation

N-Octanoyl chitosan and N-Palmitoyl chitosan and chitosan with variable concentrations were separately dissolved in 40 ml of 1% acetic acid solution and variable concentrations of sodium tripolyphosphate was dissolved in 20 ml distilled water pH 5, based on the results of preliminary study. 250 mg of Ropinirole HCl was dissolve in sodium tripolyphosphate solution and this solution was added drop-wise to N acyl Chitosan solution under continuous stirring at variable RPM (Magnetic Stirrer 1L, Remi Motors Ltd. India) at room temperature<sup>[13]</sup>.

### Optimization of Particle Size and Entrapment Efficiency by Factorial Design

Ropinirole loaded N-acyl chitosan and chitosan nanoparticle were prepared using a 3<sup>2</sup> randomized full factorial design. Accordingly, 15 possible combinations of experimental trials were prepared with three replicates. The concentration of polymer (X1) and concentration of Rif (X2) and stirring speed were selected as independent variables, while parameters mean particle size (Y1) and entrapment efficiency EE (Y2), were selected as dependent variables (response parameters). The responses were analyzed by statistical modeling of interactive and polynomial terms.

**Table 1: Levels of variables in ionotropic method for nanoparticle preparation.**

Variable	Level -1	Level -2	Level -3
N Acyl Chitosan in 40 mL (mg) in 1% acetic acid	100	300	500
sodium tripolyphosphate (mg) in 20 ml water	50	125	200
Stirring Speed (RPM)	500	1000	1500

The response surface curves and contour plots were prepared to study the effects of independent variables. All the statistical operations were carried out using Design-Expert software, version 12 (Stat-Ease Inc., Minneapolis, USA) and Microsoft Excel 2010. Independent factors at their varied combinations in terms of coded and their actual values are represented in Table 2.

Table 2: Design of experiment Parameter for Optimaization.

Batch	N Acyl Concentration (mg)	Sodium Tripolyphosphate (mg)	Stirring Speed (RPM)
A 1	300	50	1500
A 2	300	125	1000
A 3	500	125	1500
A 4	300	125	1000
A 5	100	125	1500
A 6	500	50	1000
A 7	300	125	1000
A 8	300	50	500
A 9	100	200	1000
A 10	500	200	1000
A 11	300	200	500
A 12	300	200	1500
A 13	100	50	1000
A 14	500	125	500
A 15	100	125	500

### Optimization and Data Analysis

The optimization of parameters was carried out by applying response surface methodology (RSM) computations using Design Expert® software (version 12, Stat-Ease Inc., Minneapolis, MN) and Microsoft Excel 2010. Multiple regression analysis (MLRA) was used to generate polynomial models (including interaction and quadratic terms).

Statistical validity of the polynomials was determined using ANOVA as provided in the Design-Expert® software (Stat-Ease, USA) and Microsoft Excel 2010 at a significance level of  $p < 0.05$ . In addition, 3D response surface curves, and the 2D contour plots were also developed by the Statistica® software (Stat Soft, Tulsa, USA). The best fitting mathematical model was chosen by comparing various statistical parameters such as the coefficient of variation (CV), the multiple correlation coefficient (R<sup>2</sup>), adjusted multiple correlation coefficient (Adj R<sup>2</sup>), and the predicted residual sum of squares (PRESS). For the chosen model, smaller the PRESS value in relation to the other models under consideration signifies how well the model fits the data.

### Evaluation of nanoparticles

Particle Size, Zeta Potential and PDI

The lyophilized samples were dispersed in deionised water and particle size, PDI, ZP was determined by dynamic light scattering (DLS) using Zetasizer (Malvern Instrument Ltd., UK, ZS 90) monitored at a 90° angle. All measurements were made in triplicate.

### % Drug loading (%DL) and % encapsulation efficiency (%EE)

The Ropinirole HCl loaded nanoparticles were dispersed in 10 mL of deionised water and vortexed for 5 min. The dispersion was centrifuged at 1000 rpm for 30 min and separated supernatant filtered through 0.22 µm filter (Millipore™) and analyzed at 250 nm using UV-Visible spectrophotometer (UV 2401PC, Shimadzu Corporation, Japan).

% DL and % EE were calculated using expressions previously described.

$$\% DL = \frac{\text{Amount of Ropinirole HCl in solution}}{\text{Amount of Nanoparticle}} \times 100$$

$$\% EE = \frac{\text{Amount of Ropinirole HCl in solution}}{\text{Theoretical Amount of Ropinirole added in Nanoparticle}} \times 100$$

### In vitro Mucoadhesive Study

1% (w/v) Mucin solution (1 mL) was added to each 1% w/v nanoparticle preparation (19 mL), with magnetic stirring (1L, Remi Motors Ltd. India) at 600 rpm and mixtures were incubated at 37 °C for 1 h prior to analysis. The mucin-nanoparticle mixtures were then centrifuged (C24BL, Remi Motors Ltd. India) at 1000 RPM for 60 min and 1 ml of supernatant diluted upto 10ml measured at 555 nm using UV-Visible spectrophotometer (UV 2401PC, Shimadzu Corporation, Japan) and estimate free mucin concentration using the standard calibration curve. In addition, the mucoadhesiveness was expressed as the mucin binding efficiency of the nanoparticles and was calculated from the following equation:

$$\text{Mucin Binding Efficiency}\% = \frac{C_o - C_s}{C_o} \times 100$$

Where, C<sub>o</sub> is the initial concentration of mucin used for incubation, and C<sub>s</sub> is the concentration of free mucin in the supernatant<sup>[14]</sup>.

### In vitro Drug release study

Ropinirole HCl loaded N-Acyl chitosan and chitosan nanoparticles were performed using a dialysis bag (12-14 kDa molecular weight cutoff; Himedia, India) containing 50 ml of pH 1.2 HCl and 7.4 phosphate buffer separately. Nanoparticles comprising 1 mg equivalent Ropinirole HCl were placed in the dialysis bag and both the ends were sealed. Then, the dialysis bag was kept in the receptor compartment containing dissolution medium (pH 1.2 HCl and 7.4 phosphate buffer) at  $37 \pm 0.5^\circ\text{C}$ , which was stirred at 100 rpm using a magnetic stirrer (Remi Motors, India). At regular time intervals, 0.5 ml samples were withdrawn and replaced with freshly prepared buffer upto 24 h. Analyzed by spectrophotometrically at 250 nm by using a UV-Visible spectrophotometer (UV 2401PC, Shimadzu Corporation, Japan) against the blank.

## RESULT and DISCUSSION

### Synthesis and Characterization of N Acyl Chitosan

The highly reactive acyl Chlorides were used to react with glucosamine residue of chitosan, possess reactive amino group at C-2 position to form an amide bond. Product was precipitated with acetone and dried by lyophilization for further use (Figure 1).

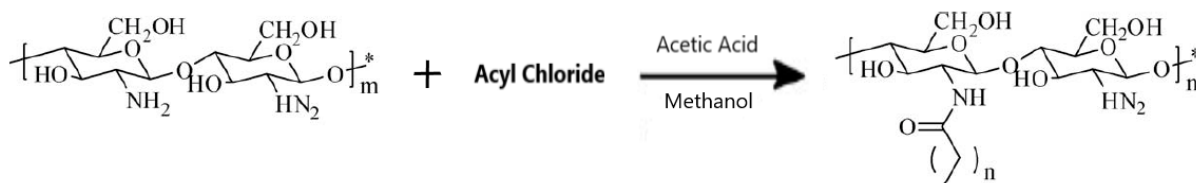


**Figure 1: Synthesis Scheme for N Acyl Chitosan.**

### IR spectroscopy N-Acyl Chitosan

The FTIR spectrum of pure chitosan exhibited the characteristic hydroxyl group absorption ( $3440\text{ cm}^{-1}$ ), along with the amide I band ( $1647\text{ cm}^{-1}$ ),  $-\text{NH}_2$  bending ( $1591\text{ cm}^{-1}$ ) and the C-O vibration ( $1026\text{ cm}^{-1}$ ), while FTIR spectra of synthesized N-Acyl chitosans observed characteristic absorption peaks at  $3000\text{--}3800\text{ cm}^{-1}$  for  $-\text{OH}$  and  $-\text{NH}_2$  stretching vibrations, and stretching vibration intensities of  $-(\text{CH}_2)_{10}-$  at  $2800\text{--}2950\text{ cm}^{-1}$  and CO stretching vibration at  $1068\text{ cm}^{-1}$ . Absorption of C-H stretching of N-Acyl chitosan at  $2918\text{ cm}^{-1}$  and  $2848\text{ cm}^{-1}$  increased with elongations of the alkyl side chain. Two major peaks at  $1662\text{ cm}^{-1}$  and  $1556\text{ cm}^{-1}$  were assigned to C=O stretching (amide I) and N-H bending vibration (amide II), respectively. Increasing amide II band in the IR spectra confirms the formation of an amide linkage between amino groups of chitosan and carboxyl groups<sup>[15]</sup>. The reaction is highly selective toward N-acylation, as it can be confirmed by the absence of a band present at  $1750\text{ cm}^{-1}$  (Figure 2). Following observations are similar with Cho et al. who studied the acylation of chitosan using Propionic acid, hexanoic acid and stearoyl acid<sup>[11]</sup>.

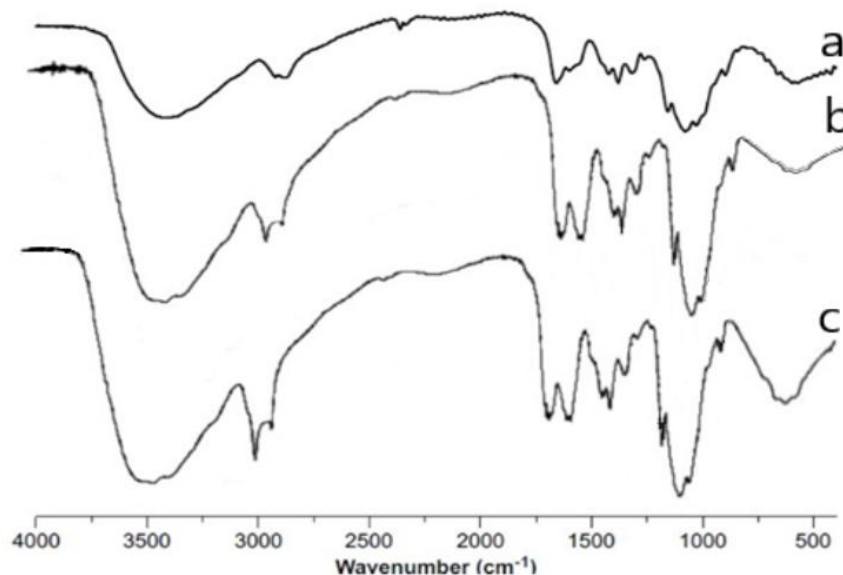


**Figure 2: FTIR Spectra a (Chitosan), b (N-Octanoyl Chitosan), c (N-Palmitoyl Chitosan).**

### NMR of N-Acyl Chitosan

Chitosan displayed two major peaks for three N-acetyl protons of N-acetyl glucosamine and the H-2 proton of glucosamine at 1.8 ppm and 2.9 ppm. The peaks at 3.1–3.9 ppm were given for (non-anomeric) ring protons of the chitosan (H-3, H-4, H-5, and H-6). The H-1 protons of the N-acetyl glucosamine and glucosamine residues were gives peaks at 4.6 and 4.8 ppm respectively.

The  $^1\text{H-NMR}$  spectrum of N-Acyl chitosan showed new peaks at 0.75 ppm for  $-\text{CH}_3$  and 0.8–1.16 ppm for proton signals of  $-\text{CH}_3$ , 1.2–1.9 for  $-\text{CH}_2-$  of acyl group, 3.0 for  $-\text{CH}_3$  of acetyl group of chitosan, 3.1–3.9 CH of carbon 2 of chitosan, CH of carbon 1 of chitosan (overlapping with the ring protons) and 4.5 ppm for  $-\text{CH}_2-$  (acyl protons) (Figure 3).

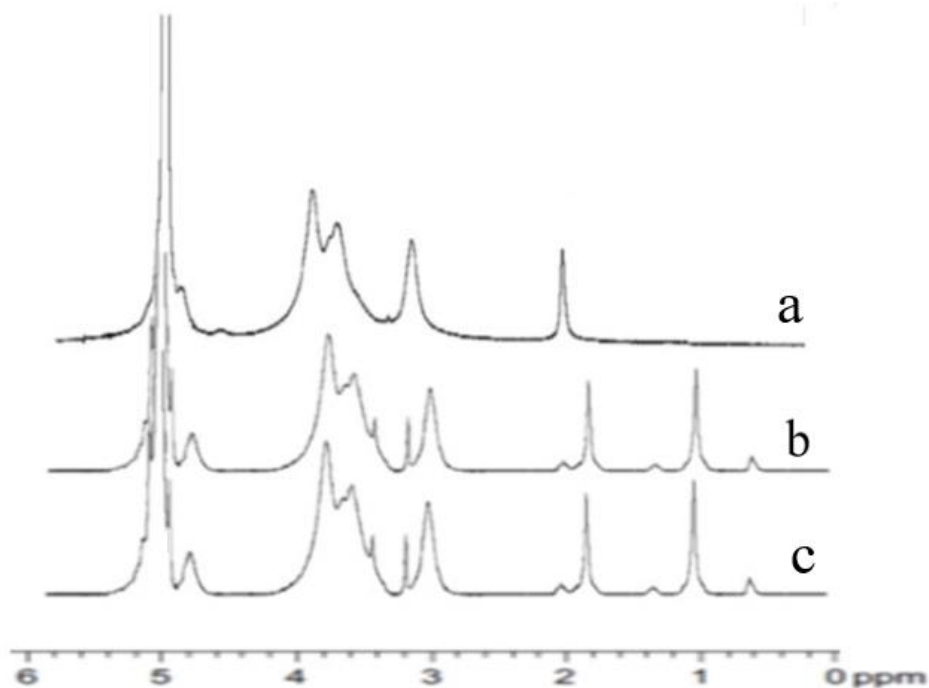
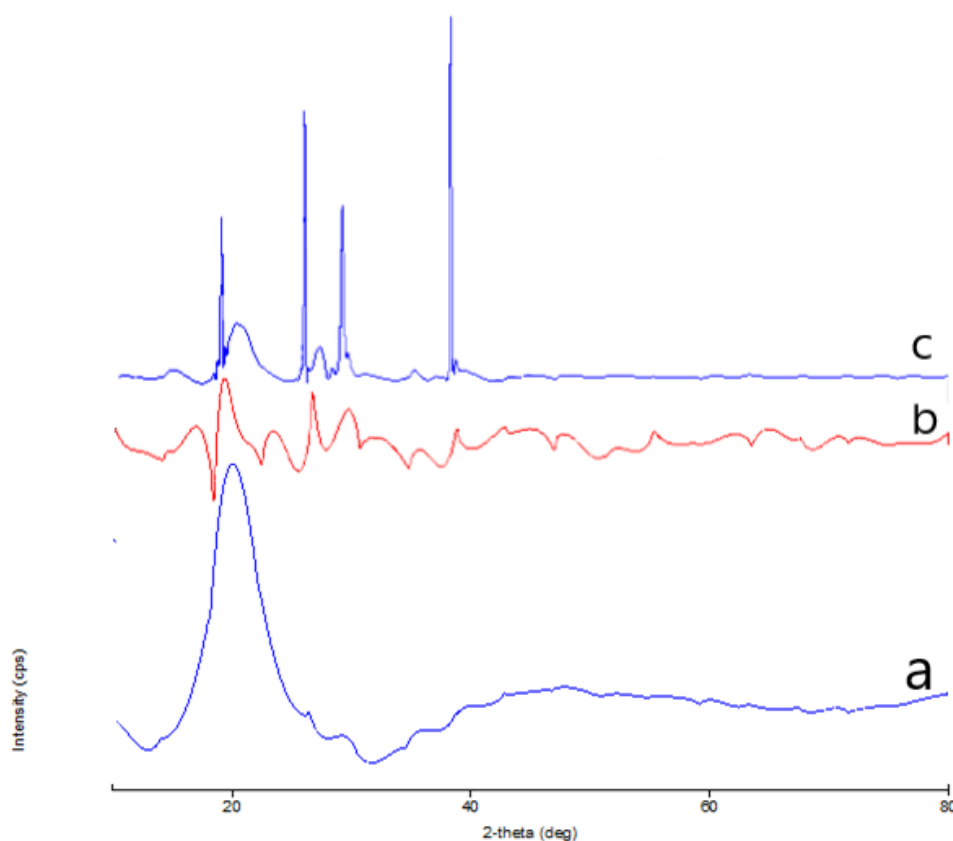


Figure 3:  $^1\text{H-NMR}$  Spectra a (Chitosan), b (N-Octanoyl Chitosan), c (N-Palmitoyl Chitosan).

### XRD of N-Acyl chitosan

Chitosan showed crystalline diffractions at  $2\theta = 20^\circ$ , while disrupted crystallinity and had been increases by the introduction of acyl substituents by modified N-Acyl chitosan (figure 4). Parallel crystallinity behavior was by Zong et al. for hexanoyl, decanoyl and lauroyl chitosan <sup>[15]</sup>.



**Figure 4: XRD of a (Chitosan), b (N-Octanoyl Chitosan), c (N-Palmitoyl Chitosan).**

### Solubility

Solubility was performed by placing 10 milligram of chitosan and N-Acyl chitosan sample into a test tube with each of 4 mL solvent. Mixing with a vortex mixer then ultrasonication, the mixture was stored at room temperature for 5 days, and visually observed as given by Ngimhuang et al. [16]. High crystallinity and strong inter or intra-molecular hydrogen bonding were responsible for poor solubility of chitosan [15]. Therefore, hydrophobic substituents into chitosan backbone may likely disrupt the inter- or intra-molecular hydrogen bonding of chitosan and weaken its crystallinity. Modified acylated chitosans showed excellent solubility in common organic solvents such as halogenated hydrocarbons and aromatic solvents, but poor solubility or swelling in polar solvents also likewise showed by Jiang et al. by stearoyl, palmitoyl and octanoyl chitosan [17].

**Table 3: Solubilities of chitosan and N acyl chitosan in various solvents.**

Solvent	Chitosan	N-Octanoyl Chitosan	N-Palmitoyl Chitosan
Water	-	+	+
Chloroform	-	+	+
Benzene	-	+	+
Toluene	-	+	+
Pyridine	-	+	+
DMSO	-	+	+
Methanol	-	+	+
Ethanol	-	+	+
Acetone	-	-	-

(+) Soluble.

(-) Insoluble

### Degree of Substitution

N-Acyl chitosans (0.3 mg) were dissolved in an aqueous acetic acid (3% w/v, 1 mL) and thoroughly stirred. Subsequently, 0.5 mL of acetic acid/acetate buffer (4 M, pH 5.5) was added into 0.5 mL of the prepared solution. Ninhydrin reagent (1 mL) was then added and solutions were placed in a boiling water bath for 20 min. Cooled and analyzed the absorbance at 570 nm using acetic acid/acetate buffer as a blank and chitosan solution was used as a control. Degree of substitution of N-Acyl chitosans was found to be 12% to 14%.

### Optimization of Particle Size and Entrapment Efficiency by Factorial Design

Influence of parameters such as concentrations of N-acyl chitosan (X1), TPP (X2) and stirring speed (X3) were optimized by applying a 3<sup>2</sup> factorial design of experiment consisting of fifteen formulation batches with random variation at three levels. Table 4 shows the combination of independent variables and observed responses in terms of mean particle size and entrapment efficiency for all the formulation.

**Table 4: Response Parameters for NPs Prepared Using 3<sup>2</sup> Factorial Design.**

Batch	Chitosan (mg)	Sod TPP (mg)	RPM	Particle Size (nm)	EE (%)
A1	300	50	1500	145.2	21.7
A2	300	125	1000	231.8	42.9
A3	500	125	1500	112.3	22.7
A4	300	125	1000	231.3	42.9
A5	100	125	1500	91.6	23.3
A6	500	50	1000	242.4	62.5
A7	300	125	1000	231.1	43.6
A8	300	50	500	206.7	36.5
A9	100	200	1000	117.5	21.5
A10	500	200	1000	109.5	23.1
A11	300	200	500	157.9	27.4
A12	300	200	1500	130.2	23.3
A13	100	50	1000	168.4	31.5
A14	500	125	500	182.3	39.8
A15	100	125	500	167.9	71.5

### Effect of Formulation Variables on the Response Parameters

Multiple regressions analysis revealed significant ( $p < 0.05$ ) influence of factors concentrations of N-acyl chitosan (X1), TPP (X2) and stirring speed (X3) on the response parameter mean particle size, while N-acyl chitosan (X1) and stirring speed (X3) were found to be statistically not significant ( $p > 0.05$ ) for % EE. The multiple regression analysis suggested quadratic models as shown in Eq. 1 and 2 for both mean particle size and EE respectively.

Particle Size =  $-55.3135 + 0.918958 * (\text{Chitosan}) + 0.893667 * (\text{TPP}) + 0.277533 * (\text{RPM}) + (-0.00136667) * (\text{Chitosan}) * (\text{TPP}) + 1.575e-05 * (\text{Chitosan}) * (\text{RPM}) + 0.000225333 * (\text{TPP}) * (\text{RPM}) + -0.00116781 * (\text{Chitosan})^2 + -0.00448667 * (\text{TPP})^2 + -0.00018465 * (\text{RPM})^2$ ------(1)

% EE=  $42.8072 + -0.0434625 * (\text{Chitosan}) + 0.437419 * (\text{TPP}) + -0.00815833 * (\text{RPM}) + (-0.0004905) * (\text{Chitosan}) * (\text{TPP}) + 7.7525e-05 * (\text{Chitosan}) * (\text{RPM}) + 7.09333e-05 * (\text{TPP}) * (\text{RPM}) + 4.57083e-05 * (\text{Chitosan})^2 + -0.00182474 * (\text{TPP})^2 + (-2.25167e-05) * (\text{RPM})^2$ ------(2)

Table 5 gives the observed and predicted values of response parameter for optimized formulation. Figure 5 for 3D surface plot for MPZ and EE while figure 6 showed overlay plot from graphical optimization. The F values for MPS and EE obtained by full model were found to be 8.1 and 1.25 respectively suggest that the model is significant. In addition, the goodness of fit of the model was established using the correlation coefficient ( $R^2$ ). The correlation coefficient ( $R^2$ ) values of MPS (0.98) and EE (0.99) showed the total variability in the model. The value of adjusted correlation coefficient (adj  $R^2$ ) for MPS was found to be 0.9358, whereas 0.6929 for EE as obtained from the full model regression analysis. The predicted  $R^2$  values of MPS and EE were found to be in reasonable agreement with the adj  $R^2$  values, suggesting statistical significance of the model, demonstrating very good correlation between the independent variables.

**Table 5: - Observed and Predicted Values of Response Parameter for optimized formulation.**

Number	Chitosan	TPP	RPM	Predicted Mean		Observed	
				Particle Size	EE	Particle Size	EE
1	102.112	150.421	519.286	151.03	55.164	150.7	54.96

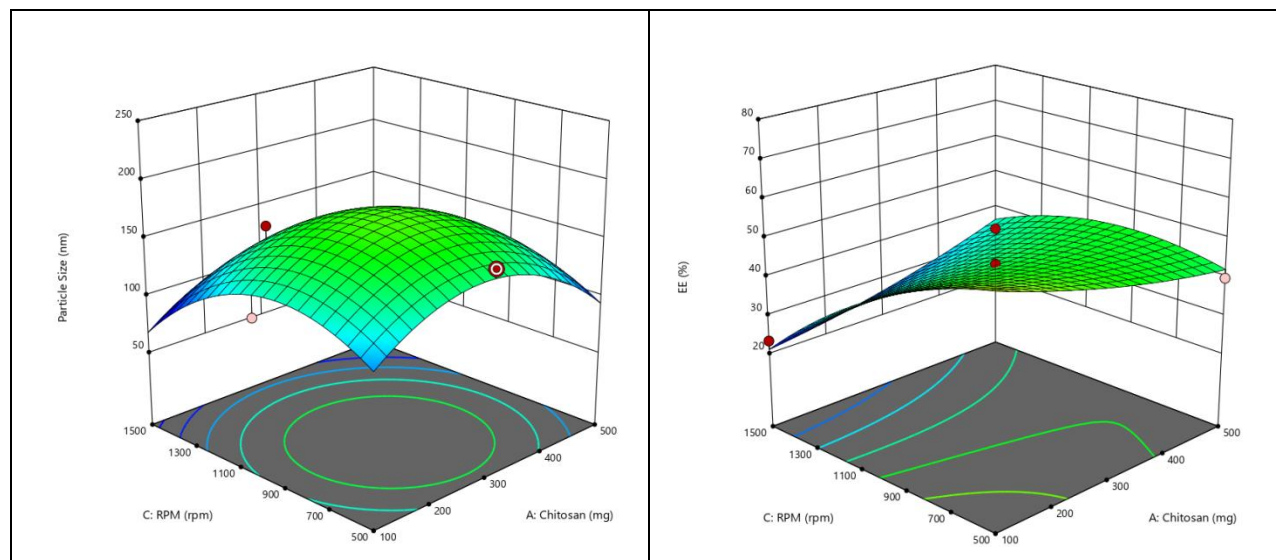


Figure 5: 3D surface plot for MPZ and EE with variable.

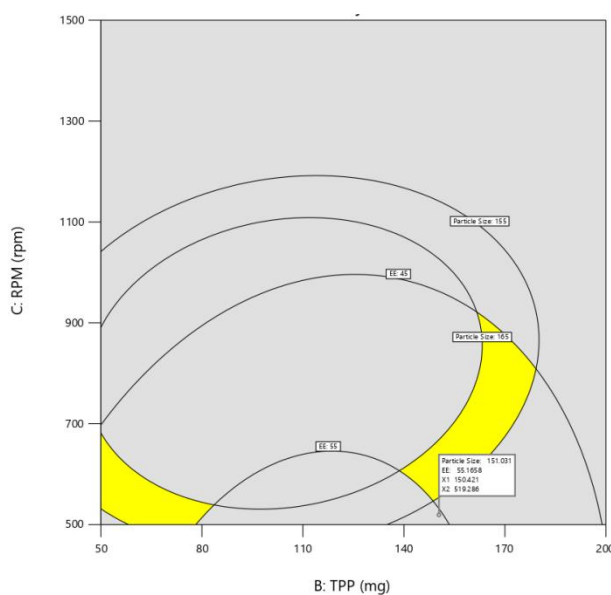


Figure 6: Overlay plot from graphical optimization.

### Particle Size, Zeta Potential and PDI

Desai and Park, prepared Protein Loading of Hexanoyl Chitosan Nanoparticles by ionotropic gelation method suggested particle size of nanoparticles ranged from 54.1 to 724.3 nm with a mean diameter of 324 nm<sup>[18]</sup>. As the length of acyl group increase with respect to average particle size also increases due to high molecular size of N-Acyl than chitosan. Cationic nature produced positive zeta potential in chitosan while N-Acyl substituted and TPP due to the charge neutralization reaction between amine groups of chitosan and negative charges of TPP decrease potential of N- acyl nanoparticle.

PDI <0.5 gives a fairly monodisperse pattern of size distribution (figure 7) by chitosan and N acyl chitosan nanoparticles. The nanosize and spherical nature with good structural integrity of the nanoparticles was confirmed by TEM and SEM analysis (Figure 8 & 9).

Table 6: Zeta Potential, Particle Size and PDI.

	Zeta Potential	Particle Size	PDI
Chitosan	11.9±0.6	150.7±3.3	0.396
N-Octanoyl Chitosan	9.4±0.8	164.4±1.4	0.447
N-Palmitoyl Chitosan	8.7±0.5	175.2±2.5	0.459

n=3.

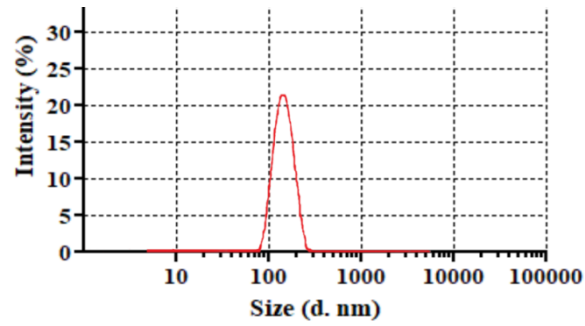


Figure 7: PDI of N Acyl Chitosan.

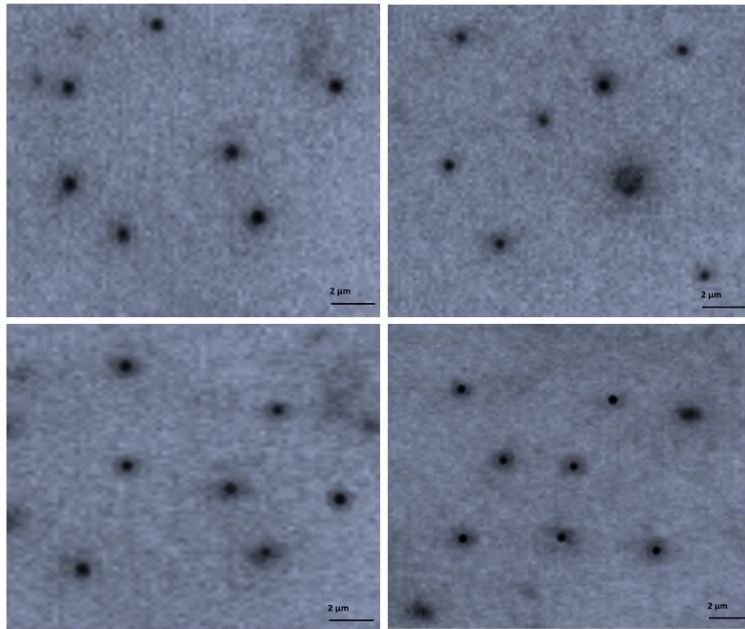


Figure 8: TEM of N-Acyl Chitosan.

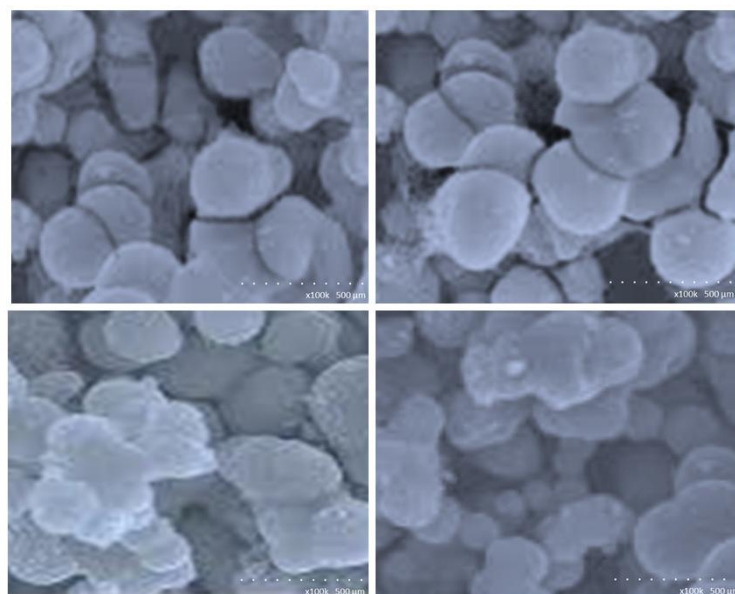


Figure 9: SEM of N-Acyl Chitosan.

### % Drug loading (%DL) and % Encapsulation Efficiency (%EE)

Either incorporation or incubation was responsible for loading drugs into nanoparticles by ionotropic method by Agnihotri et al [19]. Polyphosphate crosslinker contents, chitosan-to-drug loading ratios contribute to effects EE and DL in nanoparticle by ionotropic method demonstrated by Amidi et al [20]. Hydrophobic interactions, hydrogen bonding and other physiochemical forces was entrapment drug in nanoparticle matrix [21,22]. As the hydrophobic modification to chitosan by N-Acyl increases hydrogen bonding responsible for crosslinking indirectly drug loading capacity. Entrapment and loading was directly correlated to length of acyl group. Ropinirole HCl entrapment efficiency was increase upto  $81.26 \pm 3.4$  while drug loading was  $28.89 \pm 1.2$  as compared with chitosan (Table 7).

**Table 7: % DL and % EE of Nanoparticle.**

	% DL	% EE
Chitosan	$24.80 \pm 1.1$	$54.96 \pm 3.8$
N-Octanoyl Chitosan	$28.03 \pm 0.7$	$74.51 \pm 3.9$
N-Palmitoyl Chitosan	$30.94 \pm 0.9$	$93.51 \pm 4.3$

n=3

### In vitro Mucoadhesive Study

Mucin which distributed throughout human tissues can interact with the positive charge on the chitosan particles, due to the protonated amino group ( $\text{NH}_3^+$ ) to form electrostatic and hydrogen bonds by Hydrophobic and hydrophilic interactions [23,24].

The value of zeta potential which gives the charge was decreases as the attachment of acyl group but improvement in hydrogen bonds by hydrophobic interactions. Hence mucin binding efficiency of N-Acyl chitosan was increases with increasing the length of acyl group. *In-Vitro* mucin binding efficiency can be correlated with the mucoadhesive property of nanoparticle. N-acyl substitution increases the ropinirole HCl loaded nanoparticle mucoadhesive property which directly enhanced the permission and absorption of ropinirole through the membrane. Effect of crosslinking on the N-Acyl chitosan and chitosan was observed the similar result by Hejjaji et al., who studies the effect of various chitosan:TPP concentration on mucoadhesion of Chitosan (Figure 9) [25].

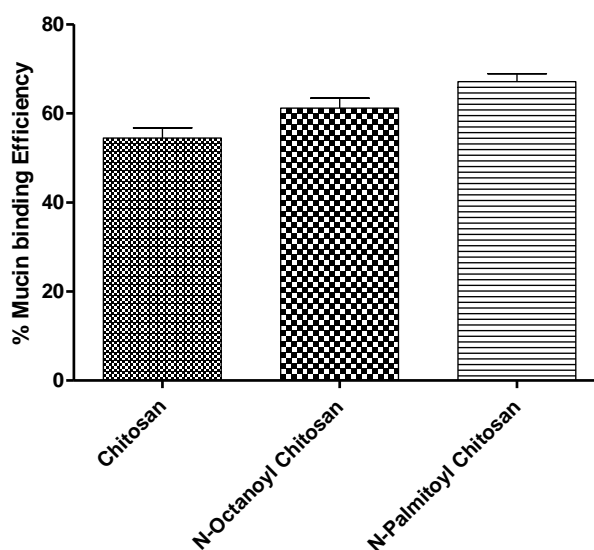


**Figure 9: %Mucin Binding Efficiency of Nanoparticle.**

### In Vitro Drug release study

N-Acyl chitosan and chitosan nanoparticles showed an initial burst release of ropinirole due to the fact that some amounts of ropinirole HCl was localized on the surface of nanoparticles by adsorption which could be released easily by diffusion. N-Acyl chitosan was retard released due to increased hydrogen bonding with drug. Burst effect diffuse the drug which are adsorbed on surface and loosely interact with polymer and resulted  $72.66\pm 1.59\%$ ,  $63.29\pm 2.04\%$ ,  $56.41\pm 1.34\%$  at pH 1.2 in 9 h while  $68.44\pm 2.98\%$ ,  $61.56\pm 3.74\%$ ,  $58.13\pm 3.47\%$  at pH 7.4 in 12 h released by chitosan, N-Octanoyl-, N-Palmitoyl nanoparticle respectively.

As the hydrophobic attached group to chitosan retard the penetration of media into core resulted drug which are present at core diffuse slowly delivered sustain released. Aqueous media penetrated into nanoparticle diffuse the drug. Hydrophobicity of N-Acyl chitosan nanoparticle increase with length of acyl group with respect to its sustain release property also enhanced as  $87.51\pm 1.52\%$  and  $79.84\pm 3.04\%$  at pH 1.2 while  $81.72\pm 2.54\%$  and  $72.03\pm 3.27\%$  at pH 7.4 ropinirole released at 24 h by N-Octanoyl-, N-Palmitoyl Chitosan respectively. While chitosan was release  $96.57\pm 3.01\%$  at pH 1.2 after 18 h and  $90.31\pm 3.64\%$  pH 7.4 after 24 h because of high solubility in acidic media due to protonation. Desai and Park observed same released pattern by protein Loading of Hexanoyl-Modified Chitosan Nanoparticles (Figure 10 & 11) [18].

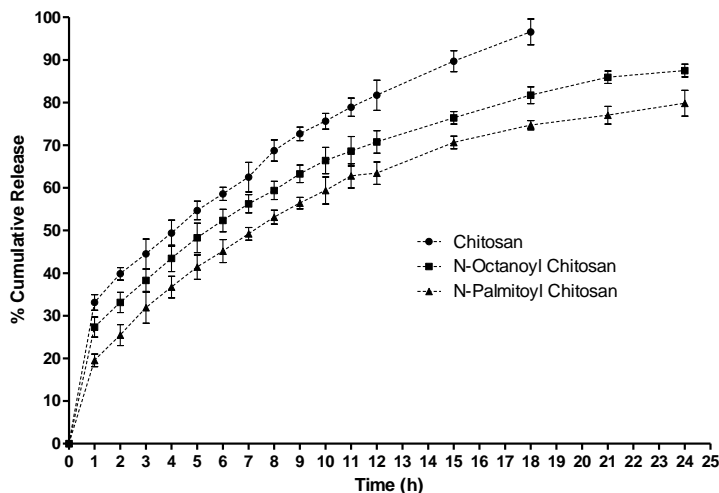


Figure 10: % Release profile at pH 1.2 of N acyl chitosan.

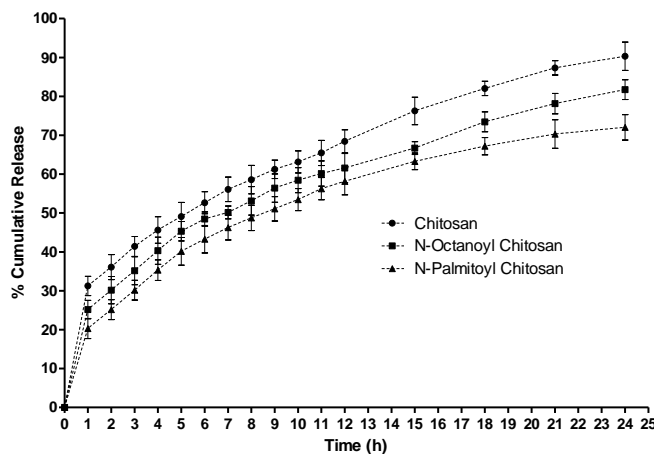


Figure 11: % Release profile at pH 7.4 of N acyl chitosan.

**Table 6: Release kinetics of N-Acyl Chitosan.**

Kinetic	Chitosan		N-Octanoyl chitosan		N-Palmitoyl chitosan	
	pH 1.2	pH 7.4	pH 1.2	pH 7.4	pH 1.2	pH 7.4
Zero order	0.5975	0.5674	0.6087	0.6095	0.5738	0.6717
First order	0.5979	0.5679	0.6091	0.6099	0.5743	0.6719
Higuchi	0.9890	0.9862	0.9900	0.9892	0.9856	0.9870
Peppas	0.9970	0.9963	0.9976	0.9962	0.9937	0.9897
Hixon-Crowell	0.5978	0.5678	0.6089	0.6097	0.5741	0.6719
Korsmeyer-Peppas	n	0.3960	0.4179	0.3768	0.4547	0.4398
	K	0.0263	0.0267	0.0267	0.0294	0.0176

Release data of N-Acyl chitosan fitting to the Korsmeyers-Peppas model demonstrated a higher value of correlation coefficient as given in table 6.  $0.5 > n$ , value for Korsmeyers-Peppas model was suggesting an fickian transport mechanism for ropinirole release by N-Butynoyl-, N-Lauroyl Chitosan and Chitosan (Table 6). This suggested that the release of ropinirole from N-Acyl Chitosan nanoparticles was not only governed by diffusion, but also included polymer swelling. Release kinetics by N-Acyl chitosan similar with Jafarieh et al. studies kinetics of ropinirole loaded chitosan nanoparticle prepared by ionotropic method<sup>[26]</sup>.

## CONCLUSION

Octanoyl and Palmitoyl Chitosan was synthesized and characterized by FTIR, NMR, XRD evaluating successful attachment of acyl group at amino position, observing the improved solubility in various solvent. Optimization of process by Factorial Design of ropinirole HCl loaded nanoparticles by ionotropic method using N-acyl chitosan and TPP. Particle size of N-Acyl chitosan nanoparticle increases with length of acyl group while decreasing zeta potential was observed. PDI exhibited uniformed monodispersed particle size also proved by TEM while SEM revealed spherical particles with smooth surfaces. The loading efficiency ranged improved upto  $30.94 \pm 0.9\%$  which directly correlated to increasing the length of N-acyl side chain. N-Acyl chitosan demonstrated sustain drug release at pH 1.2 and pH 7.4 as compared to chitosan. In Vitro exhibited the biphasic released pattern that followed Korsmeyers-Peppas model with  $0.5 > n$  value suggesting a fickian transport mechanism.

## ABBREVIATIONS

NOC = N-Octanoyl chitosan,  
 NPC = N-Palmitoyl chitosan,  
 DL = Drug loading,  
 EE = encapsulation efficiency,  
 MPS = mean Particle size

## REFERENCES

- Hassan EE, Parish RC, Gallo JM. Optimized formulation of magnetic chitosan microspheres containing the anticancer agent, oxantrazole. *Pharmaceutical Research*. 1992;9:390–397.
- Ohya Y, Takei T, Kobayashi H, Ouchi T. Release behavior of 5-fluorouracil from chitosan–gel microspheres immobilizing 5-fluorouracil derivative coated with polysaccharides and their cell specific recognition. *Journal of Microencapsulation*. 1993;10:1–9.
- Tozaki H, Komoike J, Tada C, Maruyama T, Terabe A, Suzuki T. Chitosan capsule for colon-specific drug delivery: improvement of insulin absorption from the rat colon. *Journal of Pharmaceutical Science*. 1997;86:1016–1021.
- Liu X, Chen D, Xie L, Zhang R. *J Controlled Release*. 2003;93:93.
- Harish Prashanth KV, Tharanathan RN. Chitin/chitosan: modifications and their unlimited application potential—an overview. *Trends Food Sci. Technol*. 2007;18:117.
- Wang YS, Liu LR, Jiang Q, Zhang QQ. Self-aggregated nanoparticles of cholesterol-modified chitosan conjugates as a novel carrier of epirubicin. *Eur Polym J*. 2007;43:43-53.
- Guo H, Zhang D, Li C, Jia L, Liu G, Hao L, et al. Self-assembled nanoparticles based on galactosylated O-carboxymethyl chitosan-graft-stearic acid conjugates for delivery of doxorubicin. *Int. J. Pharm*. 2013;458:31-8.
- Zhang C, Qineng P, Zhang H. Self-assembly and characterization of paclitaxel-loaded N-octyl-O-sulfate chitosan micellar system. *Colloids Surf Biointerfaces*. 2004;39:69-75.
- Quinones JP, Gothelf KV, Kjems J, Caballero AMH, Schmidt C, Covas CP. N,O 6-partially acetylated chitosan nanoparticles hydrophobically-modified for controlled release of steroids and vitamin E. *Carbohydr Polym*. 2013;91:143-51.
- Kim JH, Kim YS, Kim S, Park JH, Kim K, Choi K, et al. Hydrophobically modified glycol chitosan nanoparticles as carrier for paclitaxel. *Journal of Control Release*. 2006;111:228-234.
- Cho Y, Kim JT, Park HJ. Preparation, Characterization, and Protein Loading Properties of N-Acyl Chitosan Nanoparticles. *Journal of Applied Polymer Science*. 2012;124:1366-1371.
- Curotto E, Aros F. Quantitative determination of chitosan and the percentage of free amino groups. *Anal Biochem*. 1993;211:240-241.

13. Zarifpour M, Hadizadeh F, Iman M, Tafaghodi M. Preparation and characterization of trimethyl chitosan nanospheres encapsulated with tetanus toxoid for nasal immunization studies. *Pharma Sci* 2013;18:193-8.
14. Andersen T, Bleher S, Eide Flaten G, Tho I, Mattsson S, Škalko-Basnet N. Chitosan in mucoadhesive drug delivery: Focus on local vaginal therapy. *Marine Drugs*. 2015, 13, 222-236.
15. Zong Z, Kimura Y, Takahashi M, Yamane H. Characterization of chemical and solid state structures of acylated chitosan. *Polymer*. 2000;41:899-906.
16. Ngimhuang J, Furukawa J, Satoh T, Furuike T, Sakairi N. Synthesis of a novel polymeric surfactant by reductive N-alkylation of chitosan with 3-O-dodecyl-D-glucose. *Polymer*. 2004;45:837-841.
17. Jiang GB, Daping Quan D, Liao K, Wang H. Preparation of polymeric micelles based on chitosan bearing a small amount of highly hydrophobic groups. *Carbohydrate Polymers*. 2006, 66, 514-520.
18. Desai KG, Park HJ. Preparation, Characterization and Protein Loading of Hexanoyl-Modified Chitosan Nanoparticles. *Drug Delivery*. 2006, 13, 375-381.
19. Agnihotri SA, Mallikarjuna NN, Aminabhavi TM. Recent advances on chitosan-based micro- and nanoparticles in drug delivery. *J Control Release*. 2004, 100, 15-28.
20. Amidi M, Mastrobattista, E, Jiskoot W, Hennink WE. Chitosan-based delivery systems for protein therapeutics and antigens. *Adv Drug Deliv Rev*. 2010, 62, 159-82.
21. Ma Z, Yeoh HH, Lim LY. Formulation pH modulates the interaction of insulin with chitosan nanoparticles. *J. Pharm. Sci.* 2002, 91, 1396-1404.
22. Tang ESK, Huang M, Lim LY. Ultrasonication of chitosan and chitosan nanoparticles. *Int. J. Pharm.* 2003, 265, 103-114.
23. Morris GA, K k SM, Harding SE, Adams GG. Polysaccharide drug delivery systems based on pectin and chitosan. *Biotechnol Genet Eng Rev*. 2010, 27, 257-284.
24. Nikogeorgos N, Efler P, Kayitmazer AB, Lee, S. Bio-glues" to enhance slipperiness of mucins: improved lubricity and wear resistance of porcine gastric mucin (PGM) layers assisted by mucoadhesion with chitosan. *Soft Matter*. 2015, 11, 489-498.
25. Hejjaji EMA, Smith AM, Morris GA. Evaluation of the mucoadhesive properties of chitosan nanoparticles prepared using different chitosan to tripolyphosphate (CS:TPP) ratios. *International Journal of Biological Macromolecules*. 2018, 120, 1610-1617.
26. Jafarieh O, Shadab Md, Ali M, Baboota S, Sahni JK, Kumari B, Bhatnagar A, Ali J. Design, characterization, and evaluation of intranasal delivery ropinirole-loaded mucoadhesive nanoparticles for brain targeting. *Drug Dev Ind Pharm*. 2014, 1-8.



54878478451200605



Submit your next manuscript to **IAJPR** and take advantage of:

Convenient online manuscript submission

Access Online first

Double blind peer review policy

International recognition

No space constraints or color figure charges

Immediate publication on acceptance

Inclusion in **Scopus** and other full-text repositories

Redistributing your research freely

Submit your manuscript at: [editorinchief@iajpr.com](mailto:editorinchief@iajpr.com)

